JOURNAL OF VIROLOGY, Sept. 1996, p. 6347–6357 Vol. 70, No. 9
0022-538X/96/$04.00+0

Localization of Human T-Cell Leukemia Virus Type 1 Tax to Subnuclear Compartments That Overlap with Interchromatin Speckles

OLIVER J. SEMMES* AND KUAN-TEH JEANG

Molecular Virology Section, Laboratory of Molecular Microbiology, National Institute of Allergy and Infectious Disease, Bethesda, Maryland 20892

Received 14 December 1995/Accepted 10 May 1996

Tax, the virally encoded activator of the human T-cell leukemia virus type 1 long terminal repeats, regulates the expression of many cellular genes. This protein has been implicated in transformation events leading to the development of adult T-cell leukemia. Because subcellular localization contributes importantly to protein function, we determined the compartment(s) within the cell in which Tax is found. Using confocal microscopy, we found that Tax localizes to subnuclear domains which overlap with structures previously identified as interchromatin granules or spliceosomal speckles. These Tax speckled structures are coincident with a subset of nuclear transcriptional hot spots. Disruption of the Tax speckled structures by heat shock revealed the existence of different populations of Tax. One population of Tax is tightly associated with nuclear speckles. A second population exists outside of the speckles and is transcriptionally active for some promoters.

Tax is a potent activator of viral transcription from the human T-cell leukemia virus type 1 (HTLV-1) long terminal repeat (LTR) (6, 12, 43). This viral protein also activates many genes that participate in cellular growth and/or activation (14, 48). One or more of these pleiotropic activities of Tax is believed to lead to immortalization of T cells (13, 47). Part of this process has been suggested to involve the induction of chromosomal damage (33) and the inhibition of DNA repair (28) in cells. The diverse abilities of Tax to regulate multiple cellular activities present an experimentally challenging model for establishing correlations between differential subcellular protein localizations as determining factors for specific function.

Of the many functions of Tax, its activity in modulating expression from the viral LTR is perhaps best studied. Activation of HTLV-1 transcription most likely involves molecular interactions of Tax with cellular factors bound to LTR enhancer elements (4, 34, 42, 63). Many cellular proteins have been shown to bind the HTLV-1 LTR (25, 38, 39, 54, 61), and direct interaction between Tax and one of these proteins, CREB, has been extensively documented (2, 19, 62). What has not been well described are cellular events that precede the molecular interactions at the promoter. Hence, whether Tax reaches a promoter is dictated first by constraints of subcellular localization (8, 31, 50, 58). Indeed, a correlation between subnuclear localization and function in transcription has been established by recent in situ visualizations of transcriptional hot spots which provide physical representations of nascent RNA synthesis (23, 49, 57). The fact that Tax capably performs many different nuclear activities raises the question of whether nuclear Tax is one homogeneous population localizing to one nuclear address or whether it is composed of microheterogeneous proteins which localize to many nuclear addresses, each potentially specifying for a different function.

In this study, we investigated the subcellular distribution of Tax in transfected and transformed cells. We present evidence that in the nucleus, Tax is present in more than one functional compartment. We suggest that differential subnuclear localization might be one mechanism used to segregate and to regulate distinct activities of Tax.

* Corresponding author. Phone: (410) 614-0595. Fax: (410) 955-8685.

MATERIALS AND METHODS

Plasmids. Plasmid constructs expressing Tax and Tax mutants (TxS29, TxN43, TxA113, and TxG320) have been described previously (44). A Tax-responsive secretable alkaline phosphatase (SAP) reporter plasmid (pU3RSAP) was constructed by inserting the complete HTLV-1 U3 and R regions (−446 to +283) upstream of the SAP cDNA in pSEAP (Clonetech). pCMVSAP was constructed by inserting the simian cytomegalovirus immediate-early enhancer and promoter sequences (27) upstream of the SAP cDNA.

Antisera. Rabbit polyclonal antisera to TATA-binding protein (TBP), CREB-1, and polymerase II (Pol II) were purchased from Santa Cruz Biotechnology. Rabbit polyclonal antiserum to HTLV-1 Tax has been described elsewhere (45). Mouse monoclonal antiserum to SC35 was a gift from Tom Maniatis (15). Mouse monoclonal antibromodeoxyuridine (anti-BrdU) was purchased from Boehringer Mannheim. Affinity-purified goat anti-rabbit–Texas red conjugate and goat anti-mouse–fluorescein isothiocyanate (FITC) conjugate were purchased from Organon Teknika. Mouse hybridomas for anti-Tax were contributed by Beatrice Langton and obtained through the NIH AIDS Reference and Reagent Program.

Preparation of cells for microscopy. Cells were seeded onto glass coverslips in 100-mm-diameter tissue culture dishes with medium (Dulbecco modified Eagle medium containing 10% fetal calf serum, 2 mM glutamine, and 100 U of penicillin-streptomycin solution per ml) and allowed to adhere overnight. Initial attachment of cells produced a 40 to 60% confluence. For standard calcium phosphate transfections (20), precipitates were removed after 16 h of incubation with cells and were replaced with fresh complete medium for 24 h. At the end of this 24-h period, cells were washed twice in phosphate-buffered saline (PBS) and then incubated with PBS containing 4% paraformaldehyde (pH 8.0) for 12 min at room temperature. The fixative was removed by three washes with PBS. The cells were permeabilized by exposure to 100% methanol for 2 min at room temperature and then rehydrated with multiple rinses in PBS. Primary antibodies were diluted in PBS containing 4% bovine serum albumin (BSA) (PBS-BSA). The antibody was beaded in a 200-μl volume on Parafilm, and the prepared coverslips were inverted onto the antibody and placed into a moisturized chamber. The primary antibody was typically reacted overnight at 4°C. To remove excess primary antibody, the coverslips were washed five times in PBS-BSA. Fluorochrome-conjugated secondary antibody was reacted in the same manner except that the incubation was for 1 h at room temperature. Excess secondary antibody was removed by five washes in PBS-BSA. The processed coverslips were then mounted onto glass slides with Mounting Medium (Sigma). The prepared slides were examined by confocal optics, using a Zeis Axiophot inverted microscope.

Suspension cells were washed twice in PBS and then resuspended in PBS at 10^6 cells per ml. An aliquot (0.5 ml) of these cells was placed onto polylysine-

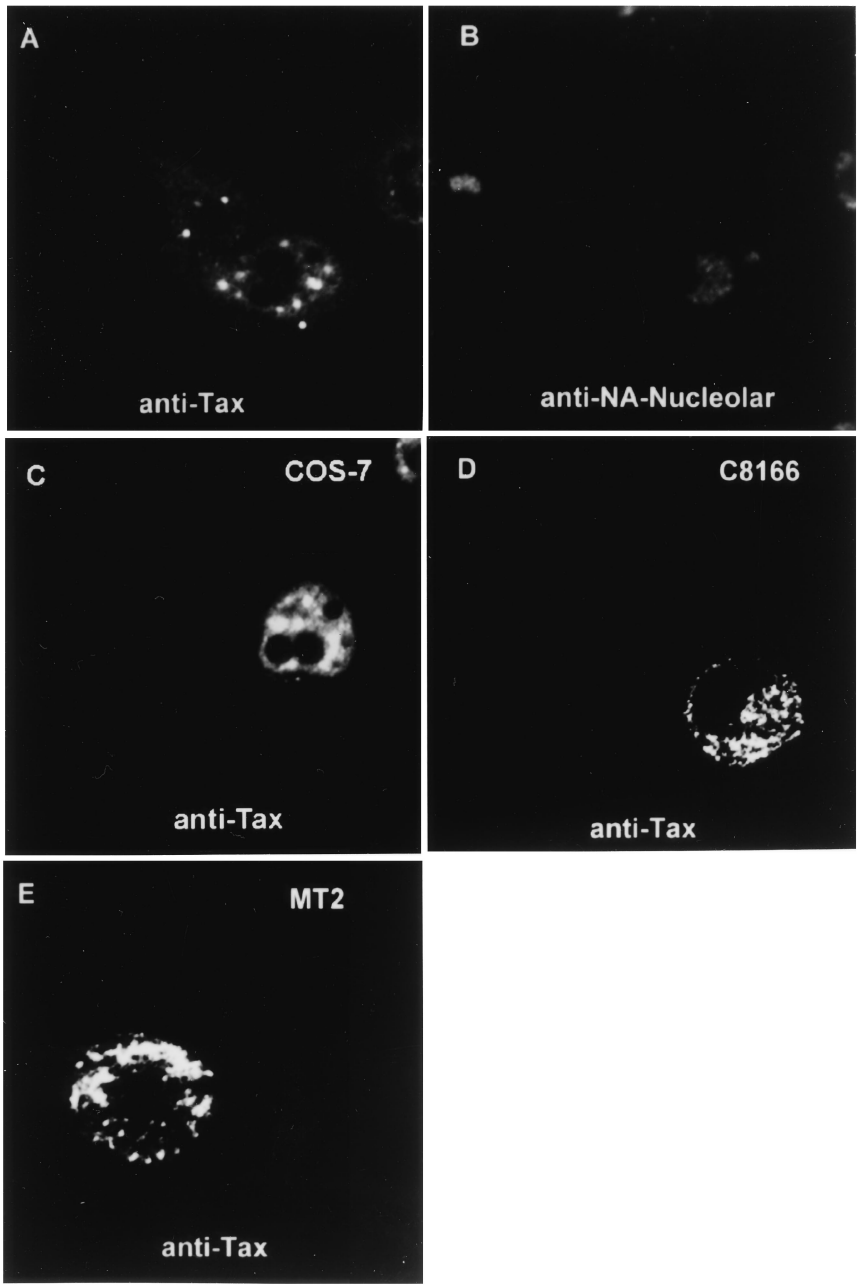

FIG. 1. Tax is found in speckled structures within the nucleus. HeLa and COS-7 cells were transiently transfected with a Tax expression plasmid. The cells were fixed, permeabilized on glass coverslips, and reacted with the appropriate primary and secondary antibodies. (A) HeLa cells stained with anti-Tax rabbit polyclonal antibody; (B) the same cells stained with anti-NA nucleolar autoimmune sera (Sigma). Secondary antibodies used were goat anti-rabbit–Texas red conjugate and goat anti-human–FITC conjugate, respectively. Note that Tax-specific fluorescence is excluded from the nucleolus and is concentrated into discrete speckles. (C) Tax-transfected COS-7 cells stained with anti-Tax. HTLV-1-transformed C8166-45 (D) and MT2 (E) cells stained with anti-Tax show the same pattern of nuclear speckles with nucleolar exclusion as seen in Tax-transfected cells. Images shown were obtained with a 64× objective lens. Variations in the cell sizes between the frames are due to slightly different printing magnifications used to produce the pictures.

coated coverslips and allowed to settle for 10 min at room temperature. The coverslips with attached cells were then washed twice with PBS and processed as described for adherent cells.

Nuclear extracts and in vitro splicing. In vitro transcription of pre-RNA and subsequent splicing in the presence of prepared nuclear extracts were performed with the RNA Splicing System (Promega). A plasmid containing the SP6 promoter and a human β-globin cDNA was used to generate RNA precursors. Synthesis and capping in the presence of [α-^{32}P]CTP to generate labeled precursor RNA were done according to manufacturer's suggestions. Excess radiolabeled nucleotide was removed by repeated precipitation in ethanol. The RNA was stored at −70°C or used immediately.

Splicing-competent nuclear extracts were prepared as previously described (30, 41). Splicing reactions were initiated by addition of 5× splicing buffer (25 mM *N*-2-hydroxyethylpiperazine-*N*′-2-ethanesulfonic acid [HEPES; pH 7.5], 100 mM creatine phosphate, 2 mM ATP, 3% polyvinyl alcohol), $MgCl_2$ to a final concentration of 2.5 mM, and β-globin pre-RNA. Reactions were halted by addition of 1% sodium dodecyl sulfate (SDS) and 10 mM EDTA. The samples were extracted once in phenol-chloroform-isoamyl alcohol (25:24:1), and the RNA was precipitated in ethanol. Pelleted RNA was dissolved into loading buffer (98% formamide, 10 mM EDTA, 0.1% xylene cyanol, 0.1% bromophenol blue) and heated at 90°C for 3 min. Splicing products were resolved by 6% polyacrylamide-urea gel electrophoresis and visualized by autoradiography.

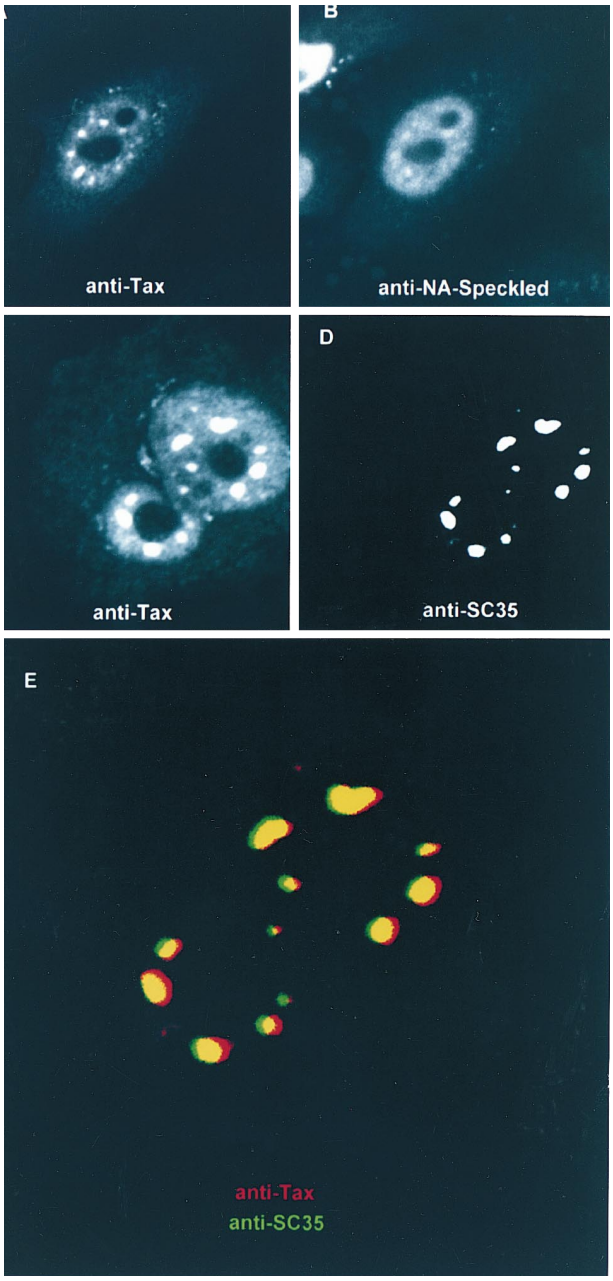

FIG. 2. Tax colocalizes with SC35. The speckled pattern of Tax staining (A) is similar to the immunostaining of the same cell with autoimmune sera (Sigma) specific for nuclear speckles (B). We compared immunostainings in the same cell with anti-Tax (C) and anti-SC35, a monoclonal antibody that recognizes one component of the proteins identified by anti-NA speckled autoimmune sera (D). Goat anti-rabbit–Texas red conjugate and goat anti-mouse–FITC conjugate, respectively, were used as secondary antibodies. When the two fluorescent signals were overlaid, very tight colocalization was observed (E). Green represents the anti-SC35 signal, and red corresponds to anti-Tax signal. Colocalization of the two entities shows as yellow. The magnification of panel E is fourfold greater than that of panels C and D.

Immunoprecipitation of SC35-containing complexes. Splicing-competent nuclear extracts were prepared as described above except that the final buffer contained 2.5 mM EDTA to block completion of RNA processing (1). Prior to immunoprecipitation, ATP was added to a final concentration of 2.5 mM. The nuclear extract (100 μl) was diluted 1:5 in splicing buffer (10 mM HEPES [pH 7.5], 50 mM KCl, 2 mM ATP) containing 2.5 mM EDTA and reacted with 50 μl of either anti-SC35 or control (anti-glutathione *S*-transferase [anti-GST]) antibody for 4 h at 4°C. The antibody complexes were captured by incubation for 1 h at 4°C with protein A beads. The beads were then washed repeatedly with splicing buffer containing 2.5 mM EDTA. Beads were solubilized by boiling in loading buffer (50 mM Tris-HCl [pH 7.0], 100 mM dithiothreitol, 2% SDS, 10% glycerol, 0.1% bromophenol blue) for 5 min. Proteins were resolved in an SDS–10% polyacrylamide gel. The proteins were then transferred to Immobilon-P filters and reacted with anti-Tax polyclonal antibody as previously described (45). Visualization of Tax-specific bands was accomplished by chemiluminescence as recommended by the manufacturer (Tropix).

In situ transcription runoff. Cells were seeded onto glass coverslips and allowed to grow to 60% confluence overnight. Some of the cells were transfected with a Tax-expressing plasmid. Both transfected and nontransfected cells were washed twice in Tris-buffered saline (10 mM Tris-HCl [pH 7.4], 150 mM $NaCl_2$, 5 mM $MgCl_2$). Tris-buffered saline was removed and replaced with glycerol buffer (20 mM Tris-HCl [pH 7.4], 5 mM $MgCl_2$, 0.5 mM EDTA, 0.5 mM phenylmethylsulfonyl fluoride, 25% glycerol) for 5 min. Cells were permeabilized with glycerol buffer containing 0.05% Triton X-100 (3 min at room temperature) and then washed once with transcription buffer (50 mM Tris-HCl [pH 7.4], 100 mM KCl, 5 mM $MgCl_2$, 0.5 mM EDTA, 1 mM phenylmethylsulfonyl fluoride, 25% glycerol, 5 U of RNasin per ml). Transcription was initiated by addition of transcription buffer containing 0.5 mM ATP, CTP, GTP, and bromo-UTP (BrUTP). Transcription was allowed to proceed for 30 min at room temperature. The reaction was halted by washing in ice-cold PBS and immediate fixation with ice-cold 100% methanol. Fixed cells were processed for microscopy as described above.

Heat shock. HeLa cells were seeded onto glass coverslips and transfected with a Tax-expressing plasmid. At 48 h posttransfection, the medium was removed and replaced with fresh complete medium prewarmed to 45°C. The cells were then maintained in a 45°C chamber for 1 h. Following heat shock, the cells were immediately fixed and prepared for microscopy.

JPX-9 cells (37) were grown to 10^6 cells per ml, and a total of 2×10^7 cells were collected by centrifugation. The cells were resuspended into 40 ml of complete medium prewarmed to 45°C. In the case of JPX-9 induced to express Tax, $CdCl_2$ was added to a final concentration of 30 μM. The cells were then incubated in a 45°C chamber with gentle rocking for 1 h.

Northern (RNA) blotting. JPX-9 cells were processed for total RNA by using the RNA STAT-60 (Tel-Test "B", Inc.) phenol-guanidinium thiocyanate method as recommended by the manufacturer. Approximately 30 μg of RNA from each sample was separated by electrophoresis in a denaturing formaldehyde-agarose gel and transferred to nitrocellulose filters. The RNA was then fixed to filter by UV irradiation and probed with [^{32}P]DNA labeled by random priming.

Secreted alkaline phosphatase (SEAP) assay. HeLa cells were seeded at 10^5/ml into six-well tissue culture plates and allowed to expand overnight. Transfection of Tax expression vector and Tax-responsive reporter was performed by using calcium phosphate. Transfection medium was removed after 16 h and replaced with fresh complete medium for 24 h. Prior to assay, transfected cells were washed three times with complete medium to remove any alkaline phosphatase produced to this point. The cells were then incubated in fresh complete medium for 1 h at 37°C. An aliquot (100 μl) of the medium was removed to assay for soluble alkaline phosphatase. For some samples, heat shock was initiated by adding complete medium prewarmed to 45°C, and the cells were placed in a 45°C chamber for 1 h. At the end of this time period, a 100-μl aliquot was removed to assay for the production of soluble alkaline phosphatase. The detection of soluble alkaline phosphatase was by chemiluminescence as suggested by the manufacturer (Clonetech). The chemiluminescent substrate was quantitated with a luminometer.

RESULTS

Tax localizes with spliceosomal speckled structures. Tax is a phosphoprotein (26) expressed in the nuclei of infected cells (17, 24). Details of the subnuclear localization(s) of Tax are unclear. To explore this issue, we visualized Tax by indirect immunofluorescence aided by confocal optics. We observed that in transfected cells, Tax is excluded from the nucleolus and is distributed in a nuclear speckled pattern. For simplicity of reference, we termed the Tax-containing speckles Tax speckled structures (TSS). Figure 1A shows TSS in HeLa cells expressing Tax. Exclusion of Tax from the nucleolus is seen in comparing Tax staining (Fig. 1A) with the staining pattern produced by nucleolus-specific antibodies (Fig. 1B) in the same cell. Reproducible TSS patterns were seen when Tax was visualized in other cell types such as COS-7 cells (Fig. 1C) and HTLV-1-transformed C8166-45 (Fig. 1D) and MT2 (Fig. 1E) T cells.

The pattern of speckling seen with TSS (Fig. 2A) resembles

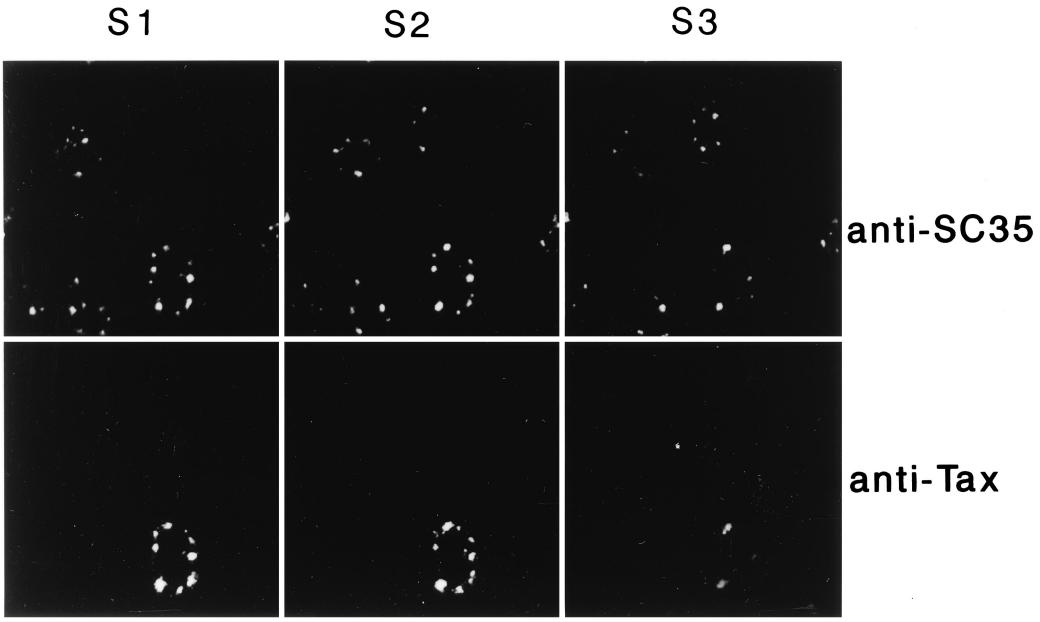

FIG. 3. Assessment of colocalization patterns by horizontal sectioning of immunostained cells. HeLa cells were costained with anti-Tax polyclonal and anti-SC35 monoclonal antibodies. The top set of each paired image is SC35-specific staining; the bottom set of each pair corresponds to Tax-specific staining. The horizontal axis of the viewing plane was digitally sectioned by 0.5-μm increments. The sequential views are labeled S1, S2, and S3. This type of sequential sectioning verifies that the colocalization of two proteins occurs in a three-dimensional manner and is not an artifact of fortuitous overlay of signals when objects are viewed in a two-dimensional plane.

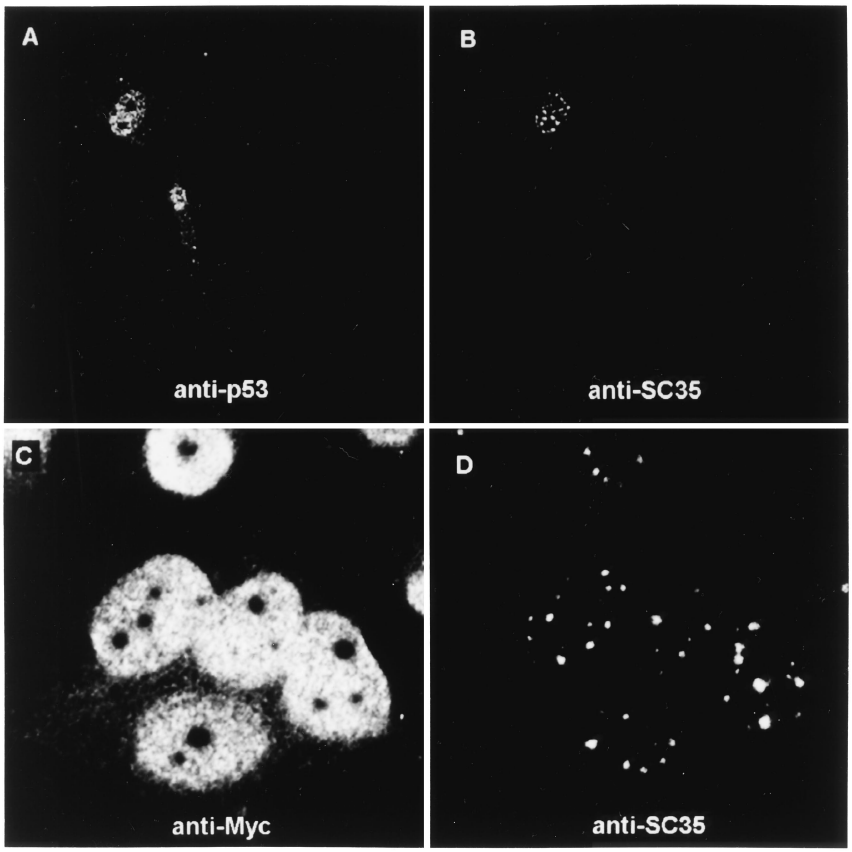

FIG. 4. SC35 does not colocalize with p53 or Myc. (A) HeLa cells (magnification, ×0.77) were stained with anti-p53 polyclonal antibody; (B) the same cells were costained with anti-SC35 monoclonal antibody. (C) COS-7 cells (magnification, ×3.9) were stained with anti-Myc polyclonal antiserum; (D) the same cells were costained with anti-SC35 monoclonal antibody. Note the different staining patterns seen with these nuclear proteins.

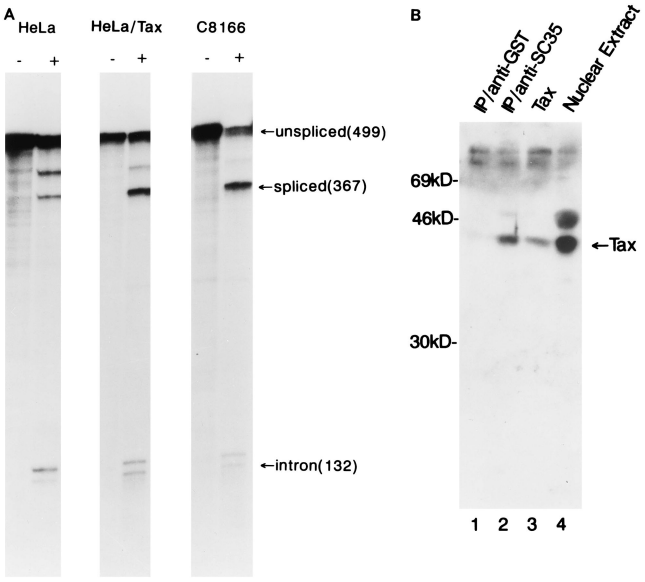

FIG. 5. Identification of Tax in SC35-containing complexes by coimmunoprecipitation. (A) Preparation of splicing-competent nuclear extracts. Splicing-competent nuclear extracts were prepared from HeLa cells (HeLa), HeLa cells expressing Tax (HeLa/Tax), and HTLV-1 transformed T cells (C8166). In each panel, splicing is compared in the presence (+) and absence (−) of the indicated nuclear extract. The input radiolabeled 499-nucleotide unspliced β-globin pre-RNA is indicated. The 367-nucleotide spliced RNA product and the excised intervening 132-nucleotide intron are also identified. Additional observed bands were not identified but may represent aberrant forms and/or breakdown products. (B) Coimmunoprecipitation of SC35-containing complexes with Tax. Splicing extracts were prepared from C8166 cells under conditions that block splicing subsequent to formation of the 60S complex. Under these conditions, multiprotein complexes containing SC35 can be immunoprecipitated (IP) with anti-SC35 (1, 15, 41). These complexes were separated by SDS-polyacrylamide gel electrophoresis and transferred to Immobilon-P filters. Western blot (immunoblot) analysis using rabbit polyclonal anti-Tax antibodies revealed the presence of Tax in these multiprotein complexes (lane 2). Tax did not precipitate when a neutral antibody (anti-GST) was used (lane 1). The presence of Tax in the C8166 nuclear extracts (lane 4) and the SC35-associated immunoprecipitates (lane 2) was verified by comparison with immunopurified Tax (lane 3). Reference molecular masses and the Tax-specific band (Tax) are indicated.

that seen when cells are stained with autoimmune antibodies to nuclear speckled antigens (Fig. 2B). One portion of the epitope population(s) recognized by anti-nuclear antigen (NA) speckle are proteins involved in splicing (53). As a direct comparison, we checked the staining pattern of TSS with that seen in the same cells stained with anti-SC35, an antibody that recognizes one component of an active spliceosome (15). When transfected HeLa cells were stained simultaneously with anti-Tax (Fig. 2C) and anti-SC35 (Fig. 2D), we observed a striking colocalization of the two signals (Fig. 2E).

One has to be cautious with visual colocalizations since signals from three-dimensional structures are often fortuitously overlaid on top of each other when viewed in a two-dimensional plane. To verify that the colocalization between Tax and SC35 was tightly linked in a three-dimensional manner, we sequentially sliced the colocalized image in a third dimension (depth) (Fig. 3). Coincidental overlays of signals would be dissociated by this approach, whereas tight physical associations between two proteins would be maintained throughout the sectioning. Images from horizontal sectionings (Fig. 3) confirmed that Tax and SC35 indeed occupy the same three-dimensional nuclear space. As a further control for specificity, we stained cells for SC35 and costained the same cells for nuclear proteins p53 (Fig. 4A and B) and c-Myc (Fig. 4C and D). In neither case did p53 or Myc localize with SC35 in the manner observed for Tax.

Tax coimmunoprecipitates with SC35-containing complexes. To confirm biochemically the presence of Tax in speckled complexes, splicing-competent nuclear extracts were made from HeLa cells, Tax-transfected HeLa cells, and HTLV-1-transformed C8166-45 cells. Each extract was verified to be active for splicing by using exogenously added β-globin pre-mRNA (Fig. 5A). We queried whether Tax would coimmunoprecipitate with components of spliceosomes that are recovered by using anti-SC35 (1, 15, 41). We immunoprecipitated Tax-expressing cellular extracts with anti-SC35 antibody under conditions that preserved the integrity of the 60S spliceosomal complex (1, 15, 41). Tax was identified by immunoblotting in the multiprotein complex captured by anti-SC35 (Fig. 5B, lane 2), supporting a tight association between Tax and spliceosomal speckled structures. In control precipitations, no Tax was detected in proteins precipitated with an unrelated anti-GST monoclonal antibody (Fig. 5B, lane 1). In other experiments, we found that anti-SC35 does not cross-recognize Tax (data not shown). Hence, these biochemical results confirm and extend the interpretation from the immunofluorescent images (Fig. 2) that Tax is found physically associated with a multiprotein nuclear structure identified by anti-SC35 antibody.

TSS overlap with regions of transcriptional activity. Because Tax is an activator of transcription, its association with spliceosomal speckles might suggest that these nuclear speckles have significance as locales of RNA synthesis. To examine this, we visualized active sites of transcription within the nucleus by using an in situ transcription runoff technique designed to identify nascent transcripts (23). Newly formed transcripts were labeled by a short pulse of BrUTP directly permeabilized into cells. The cells were then fixed immediately, immunostained with anti-BrdU (which cross-recognizes incorporated BrUTP), and examined by confocal microscopy.

Cells stained with anti-Tax (Fig. 6A) showed the typical TSS pattern. The foci of transcription in these cells were identified by simultaneous staining with anti-BrdU (Fig. 6B). Remarkably, the two stains revealed significant overlaps (Fig. 6C), suggesting that some TSS indeed represent active sites for transcription. Because TSS are also stained by anti-SC35 (Fig. 2), these areas may also be sites where transcription and splicing functionally coexist. Thus, while many nuclear speckles (according to some suggestions [18, 29, 50]) might serve as storage structures, some are clearly active spots of nascent RNA synthesis. Our findings also provide a first in situ illustration of the direct localization of Tax to transcription hot spots. That these identified hot spots truly represent sites of promoter activity was supported by control stainings for factors known to be involved in basal transcription. Using the appropriate antibodies, we confirmed that RNA Pol II (Fig. 6D to F), TBP (Fig. 6G to I), and CREB (Fig. 6J to L) all localized to the hot spots identified by anti-BrdU.

CREB/ATF-active Tax proteins target to TSS. We checked for the conformational requirements needed for Tax to target to TSS. To examine this issue, we assessed the subnuclear localization(s) of some previously described Tax mutants (44). The mutant proteins segregated into two groups, one being able to activate promoters containing CREB/ATF enhancer elements (e.g., the HTLV-1 LTR) and the second being active for NF-κB-responsive promoters (e.g., the human immunodeficiency virus type LTR).

Wild-type and mutant Tax expression vectors were transfected individually into HeLa cells. Cells were doubly stained (anti-Tax and anti-SC35), and images were visualized for Tax (Fig. 7, left column), for SC35 (Fig. 7, middle column), and for

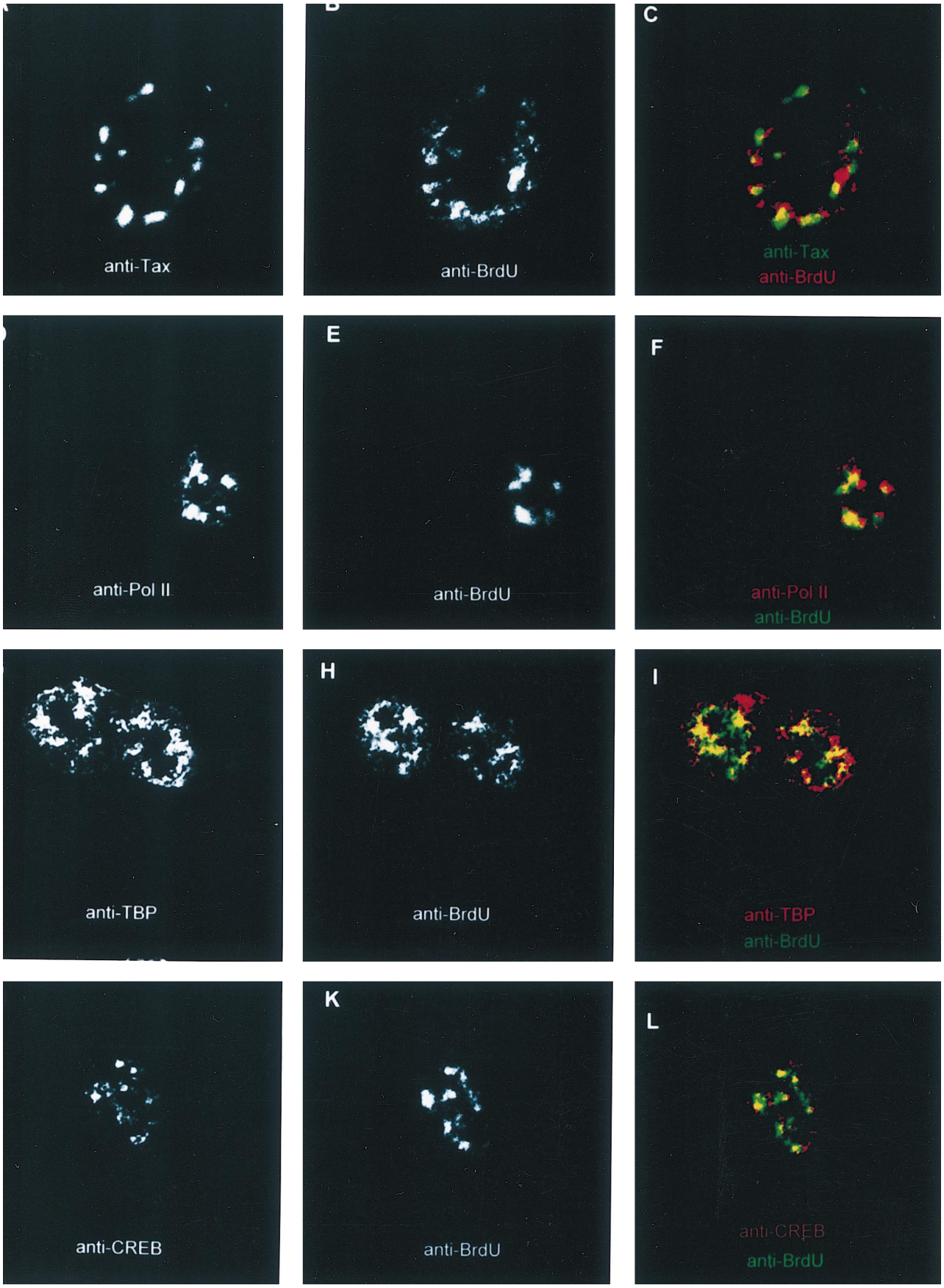
anti-Tax
anti-BrdU
C
anti-Tax
anti-BrdU
anti-Pol II
E
anti-BrdU
F
anti-Pol II
anti-BrdU
anti-TBP
H
anti-BrdU
I
anti-TBP
anti-BrdU
anti-CREB
K
anti-BrdU
L
anti-CREB
anti-BrdU

light-field morphology (Fig. 7, right column). We found that all versions of Tax localized to the nucleus and were nucleolus excluded. However, wild-type Tax (Tax [Fig. 7A to C]) and CREB/ATF-active Tax mutants (TxN43 [Fig. 7G to I] and TxA113 [Fig. 7J to L]) formed TSS, whereas CREB/ATF-inactive but NF-κB-active Tax mutants (TxS29 [Fig. 7D to F] and TxG320 [Fig. 7M to O]) stained outside of TSS. It should be noted that TxS29 and TxG320 are transcriptionally active, albeit not through the CREB/ATF pathway. Thus, TSS localization is not broadly specified by overall activity in transcription but is more narrowly defined by forms of Tax protein capable of activating CREB/ATF.

As an additional control, we verified the relative amounts of protein expressed from each form of Tax visualized in Fig. 7. Portions of the same transfected cells were normalized for cell numbers and were analyzed for expression by immunoblotting. The results support the notion that the ability of Tax to form TSS is not dependent on the relative amounts of expressed protein. Note that two Tax mutants unable to form TSS show quite different levels of expressed protein (compare Fig. 8, lanes TxS29 to TxG320, with Fig. 7D and M).

Disruption of TSS by heat shock. Incubation of cells for short times at 45°C (heat shock) has been shown to inhibit splicing by functionally disrupting spliceosome complexes that contain U1, U2, U4, U5, and U6 (9, 32, 46, 56, 60). Microscopically, heat shock perturbs the formation of nuclear speckles (5, 7, 51). We exposed Tax-expressing HeLa cells to elevated temperature in order to determine if this affected TSS. Before heat shock, Tax (Fig. 9A) and SC35-containing speckles (Fig. 9B) colocalized tightly (Fig. 9C). However, after temperature elevation, Tax (Fig. 9D) stained diffusely in the nucleus (Fig. 9F), with little coincident staining of SC35-containing complexes (Fig. 9E). The heat shock effect was transient, and reduction to normal temperature leads to recovery of TSS within 1 to 2 h (data not shown).

The disruption of TSS by heat shock provides a means for exploring whether the intactness of these structures is critical to certain Tax function. In this setting, we devised a measurement of Tax activity on transcription. We constructed a Tax-responsive SAP reporter (pU3RSAP). Expression of this reporter allowed for determination of Tax activity over short periods of time by sampling SAP in cultured cell medium. To measure SAP secretion over unit time, all preexisting SAP was removed from the culture by prior washing (twice) with fresh medium. Transfected cells were then assayed under various conditions over 1-h intervals.

Cells transfected with pU3RSAP showed a moderate increase in activity when heat shocked (Fig. 10A; compare bars 1 and 2). This was a nonspecific phenomenon, since a similar increase was also seen with pCMVSAP (Fig. 10A; compare bars 5 and 6). Cotransfection of Tax with pU3RSAP resulted in a significant increase in expression at 37°C (Fig. 10A; compare bars 1 and 3). Interestingly, Tax-activated expression was observed even at 45°C (Fig. 10A; compare bars 2 and 4), although the fold activation was slightly less than at 37°C. This Tax activity at 45°C was further confirmed by direct primer extension analysis of mRNA synthesis from pU3RSAP (Fig. 10C). Because activation of pU3RSAP by Tax is mediated through CREB/ATF, this finding indicates that a part of this function is preserved despite disruption of TSS.

To confirm TSS-independent activity in a second assay, we used the JPX-9 (37) cell line (in which Tax expression is inducible with $CdCl_2$) to measure the transcriptional activity of Tax on an endogenous cellular gene. The expression of several cellular genes, including c-*jun*, is upregulated by Tax (16). We quantitated changes in c-*jun* mRNA production in JPX-9 cells as a measure of Tax activity during heat shock. Total RNA was isolated from four treatment groups: (i) JPX-9 cells incubated at 37°C (Fig. 10B, lane 4), (ii) JPX-9 cells incubated at 45°C for 1 h (Fig. 10B, lane 3), (iii) JPX-9 cells treated with 30 μM $CdCl_2$ and incubated at 37°C (Fig. 10B, lane 2), and (iv) JPX-9 cells treated with $CdCl_2$ and kept at 45°C (Fig. 10B, lane 1). Northern blot analysis of the isolated RNAs showed an increase in c-*jun* mRNA at 37°C (Fig. 10B; compare lanes 2 and 4) upon induction of Tax by $CdCl_2$. Consistent with the pU3RSAP results, Tax activated c-*jun* transcription even at 45°C (Fig. 10B; compare lanes 1 and 3). How Tax regulates the c-*jun* promoter is unclear, but evidence suggests that this might not occur through CREB/ATF (3). Thus, this observation could represent a further example of a CREB/ATF-independent transcriptional activity of Tax that does not require TSS formation (see also Fig. 7).

DISCUSSION

It is reasonable to consider that cellular functions are not categorized simply by nuclear and cytoplasmic separations and that subcompartmentalization within these two domains could be important determinants of activity. While the physical nature of subcompartmentalization remains unclear (8, 21, 31, 50, 58), it does appear that cellular functions and proteins involved in function can in some cases be assigned to identifiable subregions in the nucleus/cytoplasm. Viral proteins produced from infection of cells should necessarily conform to the same rules dictating localization. In this study, using confocal microscopy and functional assays, we found that HTLV-1 Tax is distributed to more than one subnuclear address. While the majority of Tax is visualized as speckled bodies, which we termed TSS, some Tax function can be attributed to protein localized outside of these structures.

One set of nuclear speckles has been characterized to be involved in storage of splicing factors (18, 29, 50) and is composed of interchromatin granules and perichromatin fibrils (51, 52). In characterizing nuclear speckles, we found that Tax is associated with some of these nuclear bodies, which react with anti-SC35. One explanation for the presence of Tax in these speckles is the demonstration that some of these regions are hot spots for nascent RNA synthesis (Fig. 6). Thus, the in situ presence of Tax in hot spots provides one confirmation of its direct role in transcription and agrees with other studies that link hot spots and nuclear speckles (10, 11, 22, 23, 49, 51, 57) as sites of transcription and cotranscriptional RNA processing.

One simple model would assign all Tax activity to protein localized within TSS. However, when we studied the dissolu-

FIG. 6. TSS overlap regions of RNA Pol II transcription. HeLa cells expressing Tax were subjected to a modified in vitro transcription runoff assay utilizing incorporation of BrUTP as a means of visualizing nascent transcripts. Tax-specific speckles (A) were compared with transcription hot spots containing nascent RNA (B). The colocalization (yellow), identified by using anti-BrdU, of these two fluorescent signals is shown in panel C (printed at sixfold-greater relative magnification). Tax-specific immunostaining is green, nascent transcripts are red, and colocalization is yellow. In panels D to L, the subnuclear localization of RNA Pol II (D), TBP (G), or CREB (J) is compared with the BrUTP-determined hot spots of transcription (E, H, and K, respectively). Colocalization of the fluorescent signals associated with active transcription and Pol II (F), TBP (I), and CREB (L) is shown (printed at fourfold-greater magnification). In these images, the subnuclear localization of the specific proteins is red, the transcription domains are green, and the colocalized signal is yellow.

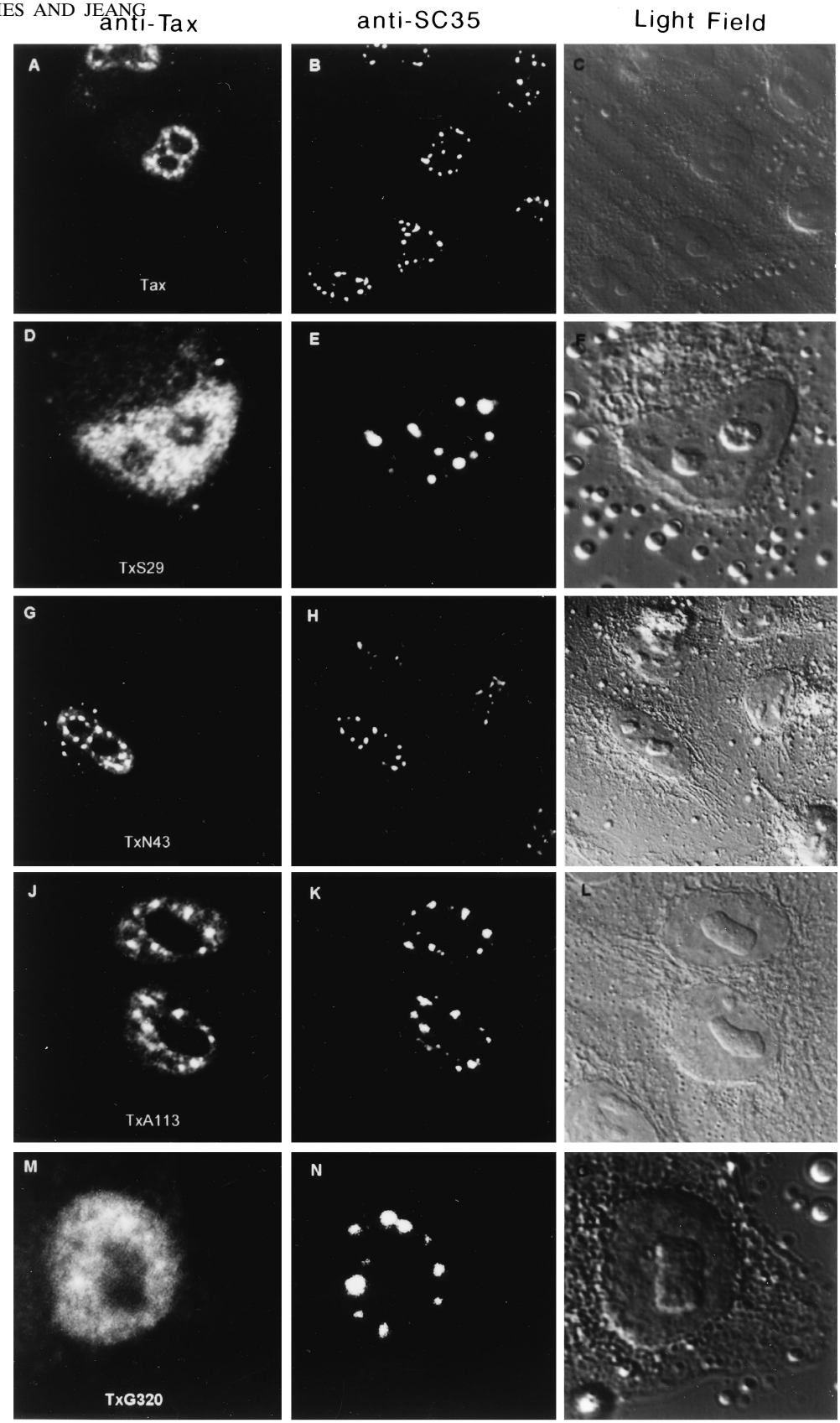

FIG. 7. CREB/ATF-active forms of Tax are found in TSS. HeLa cells were transfected with Tax (Tax) and Tax mutants (TxS29, TxN43, TxA113, and TxG320). Each Tax-expressing cell is displayed as three images of the identical field of view. Panels A, D, G, J, and M represent Tax-specific immunostaining; panels B, E, H, K, and N correspond to SC35-specific immunostaining; panels C, F, I, L, and O are light-field views. Wild-type Tax (A to C; magnification, ×1.5) and CREB/ATF-active Tax mutants (TxN43 [G to I; magnification, ×3] and TxA113 [J to L; magnification, ×4]) form distinct speckles which correspond to the anti-SC35 pattern. CREB/ATF-inactive Tax mutants (TxS29 [D to F; magnification, ×7] and TxG320 [M to O; magnification, ×7]) fail to localize in TSS and show no colocalization with SC35.

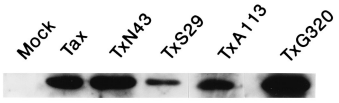

FIG. 8. Quantitation of expression of Tax and Tax mutant proteins. HeLa cells were transfected with equal amounts (5 μg) of plasmid encoding wild-type Tax or Tax mutants. Whole cell extracts were analyzed by immunoblotting using chemiluminescence-based visualization. Lanes represent mock-, Tax-, TxN43-, TxS29-, TxA113-, and TxG320-transfected cells. Each lane loading was normalized for cell numbers.

tion of TSS by heat shock (Fig. 9 and 10), this scenario could not be established. Heat stress of cells has multiple effects (59). For example, heat shock inhibits mRNA splicing (46, 59) by releasing U1, U2, U4, and U5 from the spliceosome (9, 46, 56). In our experiments, maintaining cells at 45°C for 1 h effectively prevented the visualization of TSS. However, in two separate assays (Fig. 10), TSS disruption failed to affect significantly Tax activation of an HTLV-1 LTR reporter or an endogenous c-*jun* promoter. Thus, while a portion of cellular transcription was clearly visualized to overlap with TSS (Fig. 6), and presumably this indicates some structure dependence for transcription, a part of Tax activity (as revealed by heat shock) must occur in a TSS-independent manner. This would be consistent with the pleiotropic nature of Tax function, suggesting that differential localization might be one method for determining various specificities.

Selective activation of genes is dictated through recognition of specific enhancer and transcription complexes (35, 36, 40, 55) by Tax and the delivery of Tax to the promoter. For purposes of rapid activation, TSS as passive storage sites for excess protein Tax would be functionally attractive. We cannot formally exclude that TSS, in part, might be a product of Tax overexpression; however, the findings of similar bodies in C8166-45 and MT2 cells (Fig. 1) suggest that these structures are physiologically relevant.

In general, our findings are consistent with more than one subnuclear population of Tax. We reason that some of these subsets may be for storage, others may be for CREB/ATF activation or for NF-κB and serum response factor activities, and perhaps a further set is used for transformation. We caution that these ideas of linkages between localization and specific functions are speculative and need to be confirmed by higher-resolution assays. However, at currently attainable levels of resolution, our results are supportive of the notion that spatial segregation in the nucleus contributes to one level of regulation of pleiotropic Tax functions.

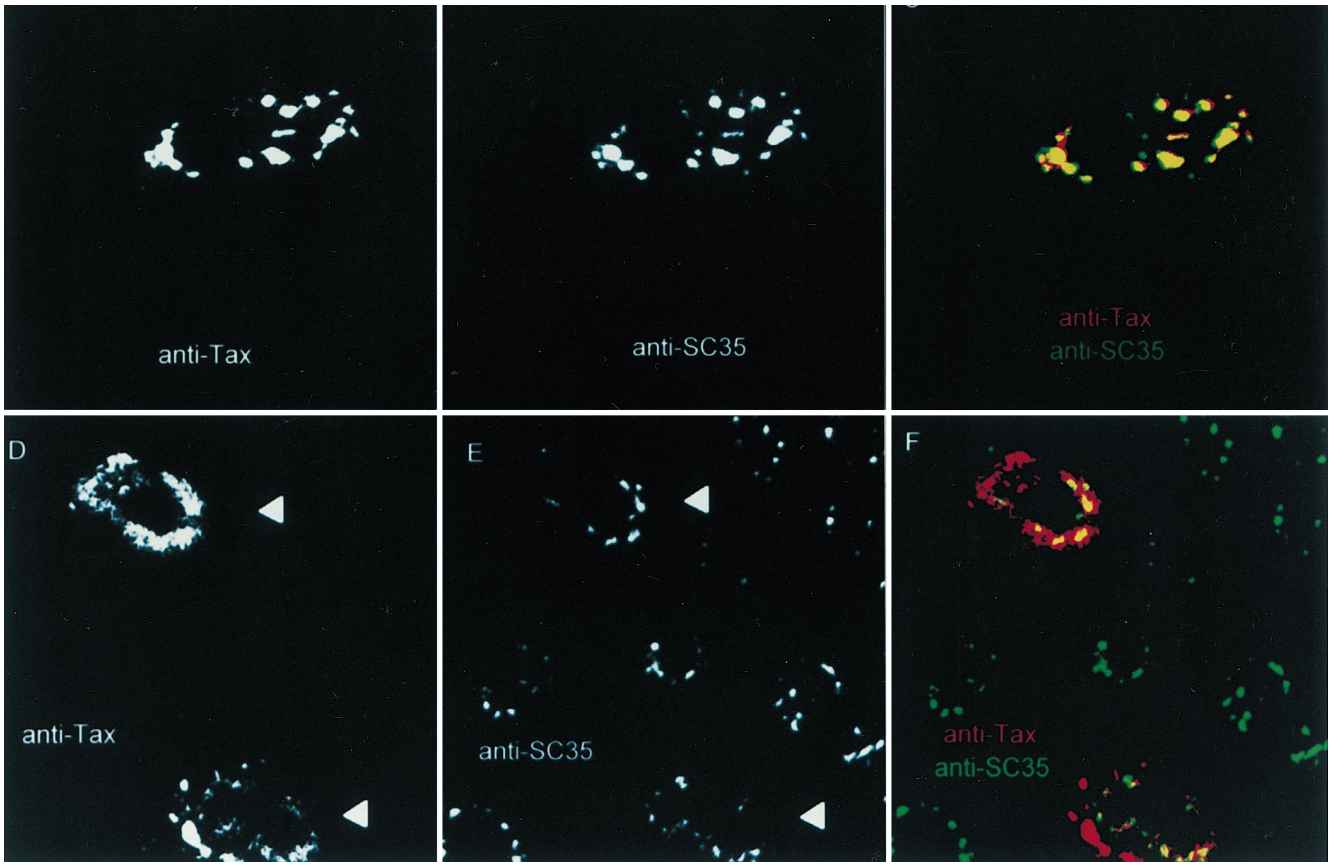

FIG. 9. Heat shock disrupts the localization of Tax into speckles. HeLa cells expressing Tax (printed at sixfold-greater magnification) were heat shocked at 45°C. Untreated cells (A to C) are compared with heat-shocked cells (D to F). In panel A, in the absence of heat shock, Tax forms distinct speckled structures that are identical to the speckles identified by anti-SC35 immunostaining of the same cell (B). In panel C, Tax-specific immunostaining is red, SC35-specific immunostaining is green, and the colocalization of the two signals is yellow. Heat shock disrupts TSS (D) and structures identified by anti-SC35 (E). Same cells in panels D and E are indicated with white triangles. In panel F, Tax-specific immunostaining is red, SC35 immunostaining is green, and colocalization is yellow.

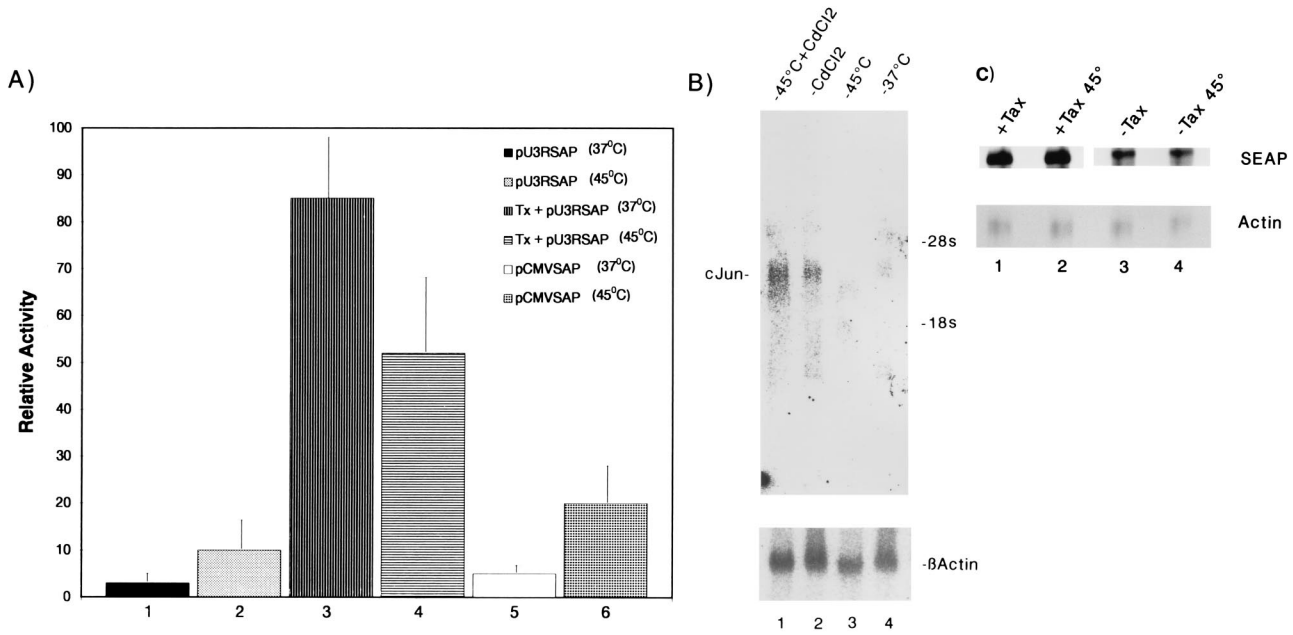

FIG. 10. Effect of heat shock on Tax-mediated transcriptional activation. Intracellular Tax activity was determined by two methods. (A) Transcriptional activation of SAP placed under the control of the HTLV-1 LTR. Transactivation by Tax was assessed by measuring alkaline phosphatase enzymatic activity secreted into the cell culture medium. Tax-mediated activation over 1 h was measured at 37°C (bar 3) and 45°C (bar 4). Basal activity of the HTLV-1 LTR was also measured at 37°C (bar 1) and 45°C (bar 2) after 1 h. As a control, the activity of a heterologous promoter, the cytomegalovirus immediate-early promoter, was measured at 37°C (bar 5) and 45°C (bar 6). (B) Transcriptional activation of c-*jun* by Tax. Inducible expression of Tax in JPX-9 cells was used to measure the induction of mRNA for c-*jun*. In the absence of Tax, there was no detectable c-*jun* mRNA at 37°C (lane 3). One hour of heat shock at 45°C also showed no c-*jun* mRNA (lane 4). Addition of $CdCl_2$ increased expression of c-*jun*. Increased c-*jun* mRNA was detected whether the cells were incubated at 37°C (lane 1) or 45°C (lane 2). β-Actin mRNA was determined for each group as a normalization for amounts of total RNA. Migration positions of 28S and 18S RNAs are indicated. (C) Analysis of SEAP mRNA by primer extension. Total RNA was isolated from cells transfected with pU3RSAP in the presence (lanes 1 and 2) or absence (lanes 3 and 4) of Tax. One set of cells was subjected to heat shock (lanes 2 and 4) prior to isolation of RNA. An oligonucleotide primer complementary to a portion of U3 at +80 was used in primer extension analysis. Shown are the relative amounts of the extended product of 98 nucleotides corresponding to the SEAP mRNA (SEAP). Increase in SEAP mRNA synthesis by Tax is the same (approximately eightfold; compare lane 3 with lane 1 and lane 4 with lane 2) at 37 or 45°C. Amounts of RNA analyzed were normalized by Northern blotting for β-actin mRNA (Actin).

ACKNOWLEDGMENTS

We thank K. Strebel and J. Hanover for critical readings of the manuscript. We are grateful to J. Coligan for peptide synthesis.

REFERENCES

1. **Abmayr, S. M., R. Reed, and T. Maniatis.** 1988. Identification of a functional mammalian spliceosome containing unspliced pre-mRNA. Proc. Natl. Acad. Sci. USA **85:**7216–7220.
2. **Adya, N., and C. Z. Giam.** 1995. Distinct regions in human T-cell lymphotropic virus type I Tax mediate interactions with activator protein CREB and basal transcription factors. J. Virol. **69:**1834–1841.
3. **Angel, P., K. Hattori, T. Smeal, and M. Karin.** 1988. The jun proto-oncogene is positively autoregulated by its product, Jun/AP-1. Cell **55:**875–885.
4. **Beraud, C., G. Lombard-Platet, Y. Michal, and P. Jalinot.** 1991. Binding of the HTLV-I Tax1 transactivator to the inducible 21 bp enhancer is mediated by the cellular factor HEB1. EMBO J. **10:**3795–3803.
5. **Beven, A. F., G. G. Simpson, J. W. Brown, and P. J. Shaw.** 1995. The organization of spliceosomal components in the nuclei of higher plants. J. Cell Sci. **108:**509–518.
6. **Cann, A. J., J. D. Rosenblatt, W. Wachsman, N. P. Shah, and I. S. Chen.** 1985. Identification of the gene responsible for human T-cell leukaemia virus transcriptional regulation. Nature (London) **318:**571–574.
7. **Carmo-Fonseca, M., R. Pepperkok, M. T. Carvalho, and A. I. Lamond.** 1992. Transcription-dependent colocalization of the U1, U2, U4/U6, and U5 snRNPs in coiled bodies. J. Cell Biol. **117:**1–14.
8. **Carter, K. C., and J. B. Lawrence.** 1991. DNA and RNA within the nucleus: how much sequence-specific spatial organization? J. Cell. Biochem. **47:**124–129.
9. **Delannoy, P., and M. H. Caruthers.** 1991. Detection and characterization of a factor which rescues spliceosome assembly from a heat-inactivated HeLa cell nuclear extract. Mol. Cell. Biol. **11:**3425–3431.
10. **Dreyfuss, G., M. J. Matunis, S. Pinol-Roma, and C. G. Burd.** 1993. hnRNP proteins and the biogenesis of mRNA. Annu. Rev. Biochem. **62:**289–321.
11. **Fakan, S., G. Leser, and T. E. Martin.** 1984. Ultrastructural distribution of nuclear ribonucleoproteins as visualized by immunocytochemistry on thin sections. J. Cell Biol. **98:**358–363.
12. **Felber, B. K., H. Paskalis, C. Kleinman-Ewing, F. Wong-Staal, and G. N. Pavlakis.** 1985. The pX protein of HTLV-I is a transcriptional activator of its long terminal repeats. Science **229:**675–679.
13. **Feuer, G., and I. S. Chen.** 1992. Mechanisms of human T-cell leukemia virus-induced leukemogenesis. Biochim. Biophys. Acta **1114:**223–233.
14. **Franklin, A. A., and J. K. Nyborg.** 1995. Mechanisms of Tax regulation of human T cell leukemia virus type I gene expression. J. Biomed. Sci. **2:**17–29.
15. **Fu, X.-D., and T. Maniatis.** 1990. Factor required for mammalian spliceosome assembly is localized to discrete regions in the nucleus. Nature (London) **343:**437–441.
16. **Fujii, M., T. Niki, T. Mori, T. Matsuda, M. Matsui, N. Nomura, and M. Seiki.** 1991. HTLV-1 Tax induces expression of various immediate early serum responsive genes. Oncogene **6:**1023–1029.
17. **Furukawa, Y., M. Osame, R. Kubota, M. Tara, and M. Yoshida.** 1995. Human T-cell leukemia virus type-1 (HTLV-1) Tax is expressed at the same level in infected cells of HTLV-1-associated myelopathy or tropical spastic paraparesis patients as in asymptomatic carriers but at a lower level in adult T-cell leukemia cells. Blood **85:**1865–1870.
18. **Gall, J. G.** 1991. Spliceosomes and snurposomes. Science **252:**1499–1500.
19. **Goren, I., O. J. Semmes, K.-T. Jeang, and K. Moelling.** 1995. Amino terminus of Tax required for interaction with CREB. J. Virol. **69:**5806–5811.
20. **Graham, F. L., and A. J. van der Eb.** 1973. Transformation of rat cells by DNA of human adenovirus 5. Virology **54:**536–539.
21. **Hozak, P., A. B. Hassan, D. A. Jackson, and P. R. Cook.** 1993. Visualization of replication factories attached to nucleoskeleton. Cell **73:**361–373.
22. **Huang, S., and D. L. Spector.** 1991. Nascent pre-mRNA transcripts are associated with nuclear regions enriched in splicing factors. Genes Dev. **5:**2288–2302.
23. **Jackson, D. A., A. B. Hassan, R. J. Errington, and P. R. Cook.** 1993. Visualization of focal sites of transcription within human nuclei. EMBO J. **12:** 1059–1065.
24. **Jacobson, S., H. Shida, D. E. McFarlin, A. S. Fauci, and S. Koenig.** 1990. Circulating CD8+ cytotoxic T lymphocytes specific for HTLV-I pX in patients with HTLV-I associated neurological disease. Nature (London) **348:** 245–248.

25. **Jeang, K. T., I. Boros, J. Brady, M. Radonovich, and G. Khoury.** 1988. Characterization of cellular factors that interact with the human T-cell leukemia virus type I p40x-responsive 21-base-pair sequence. J. Virol. **62:**4499–4509.
26. **Jeang, K. T., C. Z. Giam, M. Nerenberg, and G. Khoury.** 1987. Abundant synthesis of functional human T-cell leukemia virus type I $p40^{x}$ protein in eucaryotic cells by using a baculovirus expression vector. J. Virol. **61:**708–713.
27. **Jeang, K. T., D. R. Rawlins, P. J. Rosenfeld, J. H. Shero, T. J. Kelly, and G. S. Hayward.** 1987. Multiple tandemly repeated binding sites for cellular nuclear factor 1 that surround the major immediate-early promoters of simian and human cytomegalovirus. J. Virol. **61:**1559–1570.
28. **Jeang, K. T., S. G. Widen, O. J. Semmes, and S. H. Wilson.** 1990. HTLV-I trans-activator protein, Tax, is a trans-repressor of the human beta-polymerase gene. Science **247:**1082–1084.
29. **Jimenez-Garcia, L. F., and D. L. Spector.** 1993. In vivo evidence that transcription and splicing are coordinated by a recruiting mechanism. Cell **73:**47–59.
30. **Krainer, A. R., T. Maniatis, B. Ruskin, and M. R. Green.** 1984. Normal and mutant human beta-globin pre-mRNAs are faithfully and efficiently spliced in vitro. Cell **36:**993–1005.
31. **Lawrence, J. B., K. C. Carter, and X. Xing.** 1993. Probing functional organization within the nucleus: is genome structure integrated with RNA metabolism? Cold Spring Harbor Symp. Quant. Biol. **58:**807–818.
32. **Mahl, P., Y. Lutz, E. Puvion, and J. P. Fuchs.** 1989. Rapid effect of heat shock on two heterogeneous nuclear ribonucleoprotein-associated antigens in HeLa cells. J. Cell Biol. **109:**1921–1935.
33. **Majone, F., O. J. Semmes, and K. T. Jeang.** 1993. Induction of micronuclei by HTLV-I Tax: a cellular assay for function. Virology **193:**456–459.
34. **Matthews, M. A., R. B. Markowitz, and W. S. Dynan.** 1992. In vitro activation of transcription by the human T-cell leukemia virus type I Tax protein. Mol. Cell. Biol. **12:**1986–1996.
35. **McKnight, S. L., and K. R. Yamamoto.** 1992. Transcriptional regulation, p. 237–289. Cold Spring Harbor Laboratory Press, Plainview, N.Y.
36. **Mitchell, P. J., and R. Tjian.** 1989. Transcriptional regulation in mammalian cells by sequence-specific DNA binding proteins. Science **245:**371–378.
37. **Nagata, K., K. Ohtani, M. Nakamura, and K. Sugamura.** 1989. Activation of endogenous c-*fos* proto-oncogene expression by human T-cell leukemia virus type I-encoded $p40^{tax}$ protein in the human T-cell line, Jurkat. J. Virol. **63:**3220–3226.
38. **Nyborg, J. K., and W. S. Dynan.** 1990. Interaction of cellular proteins with the human T-cell leukemia virus type I transcriptional control region. Purification of cellular proteins that bind the 21-base pair repeat elements. J. Biol. Chem. **265:**8230–8236.
39. **Nyborg, J. K., M. A. Matthews, J. Yucel, L. Walls, W. T. Golde, W. S. Dynan, and W. Wachsman.** 1990. Interaction of host cell proteins with the human T-cell leukemia virus type I transcriptional control region. II. A comprehensive map of protein-binding sites facilitates construction of a simple chimeric promoter responsive to the viral tax2 gene product. J. Biol. Chem. **265:**8237–8242.
40. **Ptashne, M., and A. A. Gann.** 1990. Activators and targets. Nature (London) **346:**329–331.
41. **Reed, R., J. Griffith, and T. Maniatis.** 1988. Purification and visualization of native spliceosomes. Cell **53:**949–961.
42. **Seeler, J. S., C. Muchardt, M. Podar, and R. B. Gaynor.** 1993. Regulatory elements involved in Tax-mediated transactivation of the HTLV-I LTR. Virology **196:**442–450.
43. **Seiki, M., J. Inoue, T. Takeda, and M. Yoshida.** 1986. Direct evidence that p40x of human T-cell leukemia virus type I is a trans-acting transcriptional activator. EMBO J. **5:**561–565.
44. **Semmes, O. J., and K. T. Jeang.** 1992. Mutational analysis of human T-cell leukemia virus type I Tax: regions necessary for function determined with 47 mutant proteins. J. Virol. **66:**7183–7192.
45. **Semmes, O. J., and K. T. Jeang.** 1995. Definition of a minimal activation domain in human T-cell leukemia virus type I Tax. J. Virol. **69:**1827–1833.
46. **Shukla, R. R., Z. Dominski, T. Zwierzynski, and R. Kole.** 1990. Inactivation of splicing factors in HeLa cells subjected to heat shock. J. Biol. Chem. **265:**20377–20383.
47. **Smith, M. R., and W. C. Greene.** 1991. Molecular biology of the type I human T-cell leukemia virus (HTLV-I) and adult T-cell leukemia. J. Clin. Invest. **87:**761–766.
48. **Sodroski, J.** 1992. The human T-cell leukemia virus (HTLV) transactivator (Tax) protein. Biochim. Biophys. Acta **1114:**19–29.
49. **Spector, D. L.** 1990. Higher order nuclear organization: three-dimensional distribution of small nuclear ribonucleoprotein particles. Proc. Natl. Acad. Sci. USA **87:**147–151.
50. **Spector, D. L.** 1993. Macromolecular domains within the cell nucleus. Annu. Rev. Cell Biol. **9:**265–315.
51. **Spector, D. L., X. D. Fu, and T. Maniatis.** 1991. Associations between distinct pre-mRNA splicing components and the cell nucleus. EMBO J. **10:**3467–3481.
52. **Spector, D. L., W. H. Schrier, and H. Busch.** 1983. Immunoelectron microscopic localization of snRNPs. Biol. Cell **49:**1–10.
53. **Tan, E. M., E. K. Chan, K. F. Sullivan, and R. L. Rubin.** 1988. Antinuclear antibodies (ANAs): diagnostically specific immune markers and clues toward the understanding of systemic autoimmunity. Clin. Immunol. Immunopathol. **47:**121–141.
54. **Tan, T. H., M. Horikoshi, and R. G. Roeder.** 1989. Purification and characterization of multiple nuclear factors that bind to the TAX-inducible enhancer within the human T-cell leukemia virus type 1 long terminal repeat. Mol. Cell. Biol. **9:**1733–1745.
55. **Tjian, R., and T. Maniatis.** 1994. Transcriptional activation: a complex puzzle with few easy pieces. Cell **77:**5–8.
56. **Utans, U., S. E. Behrens, R. Luhrmann, R. Kole, and A. Kramer.** 1992. A splicing factor that is inactivated during in vivo heat shock is functionally equivalent to the [U4/U6/U5] triple snRNP-specific proteins. Genes Dev. **6:**631–641.
57. **Wansink, D. G., W. Schul, I. van der Kraan, B. van Steensel, R. van Driel, and L. de Jong.** 1993. Fluorescent labeling of nascent RNA reveals transcription by RNA polymerase II in domains scattered throughout the nucleus. J. Cell Biol. **122:**283–293.
58. **Wansink, D. G., R. van Driel, and L. de Jong.** 1994. Organization of pre-mRNA metabolism in the cell nucleus. Mol. Biol. Rep. **20:**45–55.
59. **Welch, W. J.** 1987. The mammalian heat shock (or stress) response: a cellular defense mechanism. Adv. Exp. Med. Biol. **225:**287–304.
60. **Wright-Sandor, L. G., M. Reichlin, and S. L. Tobin.** 1989. Alteration by heat shock and immunological characterization of Drosophila small nuclear ribonucleoproteins. J. Cell Biol. **108:**2007–2016.
61. **Xu, Y. L., N. Adya, E. Siores, Q. S. Gao, and C. Z. Giam.** 1990. Cellular factors involved in transcription and Tax-mediated trans-activation directed by the TGACGT motifs in human T-cell leukemia virus type I promoter. J. Biol. Chem. **265:**20285–20292.
62. **Yin, M. J., E. J. Paulssen, J. S. Seeler, and R. B. Gaynor.** 1995. Protein domains involved in both in vivo and in vitro interactions between human T-cell leukemia virus type I tax and CREB. J. Virol. **69:**3420–3432.
63. **Zhao, L. J., and C. Z. Giam.** 1991. Interaction of the human T-cell lymphotrophic virus type I (HTLV-I) transcriptional activator Tax with cellular factors that bind specifically to the 21-base-pair repeats in the HTLV-I enhancer. Proc. Natl. Acad. Sci. USA **88:**11445–11449.